arXiv:1409.0291v1 [math.AP] 1 Sep 2014

Revisiting the method of characteristics via a convex hull algorithm

Philippe G. LeFloch[1] and Jean-Marc Mercier[2]

[1] *Laboratoire Jacques-Louis Lions & Centre National de la Recherche Scientifique, Université Pierre et Marie Curie, 4 Place Jussieu, 75252 Paris, France. Email : contact@philippelefloch.org.*

[2] *CRIMERE, 14 rue du Cambodge, 75020 Paris, France. E-mail: jeanmarc.mercier@crimere.com*

Abstract

We revisit the method of characteristics for shock wave solutions to nonlinear hyperbolic problems and we describe a novel numerical algorithm —the convex hull algorithm (CHA)— in order to compute, both, entropy dissipative solutions (satisfying all relevant entropy inequalities) and entropy conservative (or multivalued) solutions to nonlinear hyperbolic conservation laws. Our method also applies to Hamilton-Jacobi equations and other problems endowed with a method of characteristics. From the multivalued solutions determined by the method of characteristic, our algorithm "extracts" the entropy dissipative solutions, even after the formation of shocks. It applies to, both, convex or non-convex flux/Hamiltonians. We demonstrate the relevance of the proposed approach with a variety of numerical tests including a problem from fluid dynamics.

Keywords: hyperbolic equations, method of characteristics, numerical algorithm, compressible fluid

2010 MSC: 76L05, 65L05, 35L60, 35L03 August 2014

1. Introduction

The so-called 'method of characteristics' allows one to determine *smooth* solutions $u = u(t, x)$ to nonlinear hyperbolic equations. The solution formula takes the form $(u \circ S)(t, \cdot) = u_0 \circ S_0$ and is uniquely determined by the prescribed initial data of the Cauchy problem under consideration and, on the other hand, the family of characteristics $S = S(t, \cdot)$ associated with the problem. (Here, $S_0 = S(0, \cdot)$ denotes a parametrization associated with the initial data.) For nonlinear equations, this method generally fails for large times —due to the formation of shock waves. In the present paper, we demonstrate that the characteristics are still of interest *beyond the formation of shocks*, provided the method is suitably reformulated.

- In our setting, it is natural to distinguish between two notions of solutions:
  - *The entropy dissipative solutions*, which were defined in [3, 6, 5] and satisfy all relevant entropy inequalities.
  - The *entropy conservative solutions*, which satisfy *entropy equalities* and are "highly oscillating" (and represent the multivalued solutions [2].
- We exhibit here two novel formulas (see (3.5) and (3.6)), which rely on a convex hull construction. Importantly, these formulas provide us with a numerical algorithm which is presented and implemented in the present paper. It is found to efficiently compute weak solutions with shocks for both convex and non-convex flux-functions.

We present our method in the context of multi-dimensional problems for, both, nonlinear hyperbolic conservation laws and Hamilton-Jacobi equations. We discuss several important properties of the solutions and perform numerical experiments. In particular, we demonstrate numerically that we recover the entropy solutions. The present paper is concerned with the numerical aspects of our approach, while a follow-up work will provide theoretical support for our new formulation. We also emphasize that the proposed method in principle should apply to a wide variety of nonlinear problems, provided they admit a method

of characteristics. We apply it here to convex and non-convex conservation laws and to a problem of fluid dynamics. We expect our method to be applicable to other hyperbolic problems.

We work in a spatial domain Ω which is taken to be $\Omega := \mathbb{R}^D$ throughout this paper. We consider functions $u = u(t, x)$ defined for positive times $t \geq 0$ and satisfying one of the following two Cauchy problems:

- *Nonlinear conservation laws:*

$$\partial_t u + \nabla \cdot f(u) = 0, \quad u(0, \cdot) = u_0, \tag{1.1}$$

  where $f(u) := (f_d(u))_{d=1,\dots,D} : \mathbb{R} \mapsto \mathbb{R}^D$ is a given flux-function and $\nabla \cdot f(u)$ denotes the divergence $\sum_{d=1,\dots,D} \partial_{x_d} f_d(u)$.

- *Hamilton-Jacobi equations:*

$$\partial_t w + H(\nabla w) = 0,$$

  with a given Hamiltonian $H : \mathbb{R}^D \mapsto \mathbb{R}$, where $\nabla u = \{\partial_{x_d} u\}_{d=1,\dots,D} \in \mathbb{R}^D$ denotes the gradient. In fact, by introducing the unknown $u := \nabla w \in \mathbb{R}^D$, we can equivalently consider the following *system* of nonlinear hyperbolic equations:

$$\partial_t u + \nabla(H(u)) = 0, \quad u(0, \cdot) = u_0 := \nabla w_0. \tag{1.2}$$

Clearly, the constraint $u = \nabla w$, i.e. the fact that u is a gradient, is satisfied for all times provided it holds at the initial time.

The method of characteristics applies to both problems and generates a smooth solution $u = u(t, \cdot)$ for sufficiently small times $t \leq \delta$ (at least) in the following form (cf. the notation below):

$$u(t, \cdot) = (u_0 \circ S(0, \cdot)) \circ S^{-1}(t, \cdot), \quad 0 \leq t \leq \delta, \tag{1.3}$$

where the map $S = S(t, x)$ parametrizes the family of characteristics. Our main observation based on the novel notion of *convex hull transform* allows us to generalize the characteristic method to all times, by relying on two explicit formulas (cf. (3.5) and (3.6)). Since the characteristic map $S(t, \cdot)$ is onto, defining its inverse $S^{-1}(t, \cdot)$ requires some care, and this issue is addressed below.

Since our formulas are based on a reformulation of the characteristic method, the approach we propose here is very general and should apply to many nonlinear hyperbolic problems. At the end of this paper, we for instance discuss an application to fluid dynamics. Our formulas are easily implemented in numerical applications (cf. the discussion in Section 4 below) and allows us to compute solutions for all times $t \geq 0$ and for all dimensions D. The method applies to arbitrary equations like (1.1) and (1.2), including *non-convex flux-functions* f and *non-convex Hamiltonians.*

In term of efficiency, our algorithm can favorably compete with spectral techniques such as the ones proposed for nonlinear hyperbolic problems by Sidilkover and Karniadakis [10] and followers, as well as techniques where the Rankine-Hugoniot relations are directly enforced at the discrete level such as the one proposed by Jaisankar and Raghurama Rao [4]. Importantly, we expect the proposed method to generalize to many problems which admits a classical method of characteristics; for instance, problems with source-terms. Our approach could provide a robust alternative (or supplementary tool) to design well-balanced techniques, such the ones in Boscarino and Russo [1].

2. The convex hull transformation

2.1. Motivation

The present subsection provides a motivation for the present paper, but the reader unfamiliar with measure theory *can skip this subsection* and read directly the next subsection. Without genuine loss of generality, we will work with smooth and spatially decaying initial data (so that the derivatives are integrable). Let $\Lambda \subset \mathbb{R}^D$ be a convex set with unit Lebesgue measure and, typically, we can work with the unit cube $[-\frac{1}{2}, \frac{1}{2}]^D$. By unit measure, we mean that $m(\Lambda) = 1$, where m stands for the Lebesgue measure. More generally, we use the notation $\mu(\Gamma)$ for the measure of a set Γ with respect to a finite measure μ.

Let us first consider general maps $S : y \in \Lambda \mapsto x = S(y) \in \Omega$, defined on an open, bounded, and convex set $\Lambda \subset \mathbb{R}^D$ (with $D \geq 1$) and taking values in a convex and open set $\Omega \subset \mathbb{R}^D$. As usual, we denote by $\mathcal{P}(\Omega)$ the set of all positive measures on Ω with unit total mass. Given two probability measures $\mu \in \mathcal{P}(\Omega)$ and $\nu \in \mathcal{P}(\Lambda)$, we say that a map $S : \Lambda \mapsto \Omega$ is (μ, ν)–*measure preserving* (or transports ν into μ) if and only if $S_\sharp \nu = \mu$, that is, $\mu(S(A)) = \nu(A)$ for all (μ-measurable) sets $A \subset \Omega$. This condition is equivalent to the change of variable formula $\int_\Omega \varphi \, \mu = \int_\Lambda (\varphi \circ S) \, \nu$.

According to the general theory of optimal transport, given $\Omega \subset \mathbb{R}^D$ and for a positive probability measure $\mu \in \mathcal{P}(\Omega)$ satisfying $\operatorname{supp} \mu = \Omega$ and $\mu << m$ (that is, μ is absolutely continuous with respect to the Lebesgue measure), these exists a unique map $S : \Lambda \mapsto \Omega$ "transporting" the Lebesgue measure m on Λ into μ. More precisely, let $S : \Lambda \to \Omega$ be a square-integrable map and consider the probability measure $\mu := S_\# m \in \mathcal{P}(\Omega)$. Then the following decomposition

$$S = (\nabla h) \circ T, \qquad h : \Lambda \to \mathbb{R} \text{ convex}, \qquad T_\# m = m, \tag{2.1}$$

holds and is called the *polar factorization* of the map S. Here, by definition, the map T is thus Lebesgue-measure preserving.

The following remark in also in order: the convex factorization is known to be unique when the measure $S_\# m := \mu > 0$ is absolutely continuous with respect to the Lebesgue measure, but uniqueness might be lost otherwise. In the present paper, due to the presence of shock waves, this uniqueness will not necessary hold.

2.2. A novel notion

Let $S : \Lambda \to \Omega$ be a square-integrable and surjective map of the form $S = \nabla h$. Then, the *convex hull transformation* S^+ of S is defined as

$$S^+ := \nabla h^+, \quad \text{where } h^+ \text{ is the convex hull of } h. \tag{2.2}$$

In view of this definition, S^+ is also surjective and the probability measure $\mu^+ := S^+_\# m \in \mathcal{P}(\Omega)$ is in general singular, i.e. need not absolutely continuous with respect to the Lebesgue measure m on Ω and may typically contain Dirac masses. In this context, we have the following proposition which allows us to inverse the map S^+ by solving the equation $u \circ S^+ = v_0$ when v_0 is a prescribed smooth function fixed throughout.

Solving the equation $u \circ R = v_0$

Monotone maps admit generalized inverses defined as follows. Let $R : \Lambda \mapsto \Omega$ be a surjective map and consider the measure $\mu := R_\# m > 0$. Suppose $R = \nabla k$, where $k : \Lambda \to \Omega$ is convex. Given an integrable function v_0 defined on Λ, we can introduce the integrable function $u(\cdot) := v_0 \circ R^{-1}(\cdot)$ as the density of the measure $R_\#(v_0 m)$ with respect to μ. This function is defined almost everywhere and satisfies for every set A

$$(u\mu)(A) = \int_B v_0, \quad B = R^{-1}(A). \tag{2.3}$$

We omit here the discussion of the relevant regularity and functional spaces. With the convex hull transformation S^+, the function $u = v_0 \circ (S^+)^{-1}$ defined as above, satisfies (by Jenssen inequality)

$$U(u) \leq U(v_0) \circ (S^+)^{-1} \qquad \text{for every convex function } U \tag{2.4}$$

and, by definition, we then say that the convex hull transformation is *entropy dissipative.*

3. Entropy dissipative/conservative solutions

3.1. The characteristic map

Parametrization of the initial data

We begin by formulating the standard characteristic method, which can be used to compute solutions for sufficiently small times. This holds for both equations (1.1) and (1.2). Observe that our formulation is based on a specific parametrization of the initial data.

We consider either scalar-valued functions $u = u(t,x)$ or vector-valued maps $u = u(t,x) := \{u_i(t,x)\}_i$. As stated in the introduction, the gradient operator is denoted by ∇, while the divergence operator is denoted by $\nabla\cdot$). We introduce the norm $|\nabla u|_1 := \sum_i |\partial_i u|$ for any (piecewise smooth, say) function $u = u(t,\cdot)$ defined on Ω. If u is vector-valued, we write $|\nabla u|_1 := \sum_{i,j} |\partial_i u_j|$. With this notation, we are given a smooth initial data u_0 and we suppose supp $\nabla u_0 = \Omega$ so that u_0 does not have "flat part". This is not a genuine restriction and can be ensured by an arbitrary perturbation of u_0. We then introduce the *initial map*

$$\begin{aligned} &S_0 = \nabla h_0 : \Lambda \mapsto \Omega, \qquad h_0 : \Lambda \to \mathbb{R}, \text{ convex}, \\ &S_{0\#} m = \mu_0 = \frac{|\nabla u_0|_1}{|\nabla u_0|_1(\Omega)} \in \mathcal{P}(\Omega). \end{aligned} \tag{3.1}$$

We observe that S_0 is more regular (by one additional derivative) than the function $|\nabla u_0|_1$, which itself is solely continuous (with bounded derivatives).

Nonlinear conservation laws

For each time t, we define the *characteristic map* $S(t,\cdot) : \Lambda \mapsto \Omega$ for the conservation law (1.1) as :

$$S(t,\cdot) := \big(S_0 + tf'(v_0)\big) \qquad v_0 := u_0 \circ S_0, \tag{3.2}$$

which admits bounded derivatives up to first order at least.

Hamilton-Jacobi equation

Let $u_0 : \Omega \to \mathbb{R}^D$ be a smooth function, and suppose supp $\nabla u_0 = \Omega$. Consider its initial map as in (3.1). Then define the *characteristic map* $S(t,\cdot) : \Lambda \mapsto \Omega$ of the Hamilton-Jacobi equation (1.2) as :

$$S(t,\cdot) = \big(S_0 + t(DH)(v_0)\big) \qquad v_0 := u_0 \circ S_0, \tag{3.3}$$

where DH is the differential of the Hamiltonian.

Within a sufficiently small time interval $0 \le t \le \delta$, the characteristic maps above are invertible map, and provide us with solutions to both equations, via

$$u(t,\cdot) := (v_0 \circ S^{-1})(t,\cdot), \quad 0 \le t \le \delta. \tag{3.4}$$

Indeed, (3.4) defines the unique smooth solution to (1.1) and (1.2) within the interval under consideration.

3.2. A novel method of characteristics

We now introduce two explicit formulas, which provide solutions to (1.1) and to (1.2) for all positive times, i.e. beyond shock formation. Consider the characteristic maps $S(t,\cdot)$ for the conservation law and Hamilton-Jacobi equations defined in (3.2)-(3.3), suppose without restriction that $S_0 : \Lambda \to \Omega$ is square-integrable.

Entropy conservative

Consider $S(t,\cdot) = (\nabla h \circ T)(t,\cdot)$ the polar factorization of S, see (2.1), with $h(t,\cdot) : \mathbb{R}^D \to \mathbb{R}$ convex and $T : \Lambda \mapsto \Lambda$ Lebesgue measure preserving. For all positive times, we define the *entropy conservative* solution as

$$u(t,\cdot) = \big(v_0 \circ T^{-1} \circ (\nabla h)^{-1}\big)(t,\cdot) \tag{3.5}$$

for all positive times, in which the inverse $S^{-1} := T^{-1} \circ (\nabla h)^{-1}$ is well-defined since h is convex and T is measure-preserving.

Entropy dissipative

Suppose $S(t,\cdot) = \nabla h(t,\cdot)$, with $h : \Omega \to \mathbb{R}$ and consider its convex hull transform $S^+(t,\cdot)$, given earlier. We define the *entropy dissipative solution*

$$u(t,\cdot) = \big(v_0 \circ (S^+)^{-1}\big)(t,\cdot) \tag{3.6}$$

for all positive times, in which the generalized inverse S^{-1} was defined earlier. Furthermore, in the general situation $S = \nabla h \circ T$, we can introduce a more general transformation of the form $S^+ = \nabla h^+ \circ T^+$, with a (possibly non-trivial) measure-preserving map T^+, but this is unnecessary for our purpose in the present paper.

3.3. Properties of entropy dissipative solutions

We now state some properties of the entropy dissipative solutions. Consider the map $S^+(t,\cdot)$ and the function $u(t,\cdot) = v_0 \circ (S^+)^{-1}$ defined by the formula (3.6).

1. $S^+(t,\cdot) : \Lambda \to \Omega$ is continuous and surjective. For almost all $x \in \Omega$, there exists a unique $y \in \text{supp}\,(\nabla S^+)$ such that
$$x = S^+(t,y) = S(t,y). \tag{3.7}$$
2. The function $u := v_0 \circ (S^+)^{-1}$ is a weak solution to the conservation law (1.1).
3. At every point of discontinuity of u (with limits denoted by u_l, u_r), the map S^+ satisfies the Rankine-Hugoniot relations $\partial_t S^+ = \frac{[f(u\circ S^+)]}{[u\circ S^+]} = \frac{f(u_r)-f(u_l)}{u_r-u_l}$, while, at points of continuity, we can write $\frac{[f(u\circ S^+)]}{[u\circ S^+]} = f'(u\circ S^+) = f'(v_0)$ (in the support ∇S).
4. The entropy condition holds: for instance in one space dimension and at a point of discontinuity where $u_l \le u_r$ one has $\frac{f(u)-f(u_l)}{u-u_l} \ge \frac{f(u_r)-f(u_l)}{u_r-u_l} \ge \frac{f(u)-f(u_r)}{u-u_r}$ for all $u \in [u_l, u_r]$.
5. In one space dimension and for a convex flux-function, we can recover the Hopf-Lax formula: (3.6) coincides with the following formula $w(t,x) = \int_{-\infty}^{x} u(t,s)\,ds$ with $w(t,x) = \inf_z \big(w_0(z) + tf^*\big(\frac{x-z}{t}\big)\big)$, where $f^*(z) = \sup_y (zy - f(y))$ is the Legendre-Fenchel transform of the flux.

We recall that the Hopf-Lax formula allows one to compute solutions to (one-dimensional) conservation laws and (multi-dimensional) Hamilton-Jacobi equations when the flux or the Hamiltonian are convex.

4. An illustration with Burgers equation

Before we present our algorithm in full details (in the forthcoming section), we want first to illustrate our formula with a typical example. We thus consider the formulas (3.6)-(3.5) for the inviscid Burgers equation, that is, the equation (1.1) with quadratic flux-function:

$$\partial_t u + \partial_x\Big(\frac{u^2}{2}\Big) = 0, \qquad u(0,x) = u_0(x). \tag{4.1}$$

Here, we define the map $S : \Lambda = [-\frac{1}{2}, \frac{1}{2}] \to \Omega := \mathbb{R}$ by

$$S(t,\cdot) = S_0 + tv_0, \qquad S_{0,\#}m = \frac{|\partial_x u_0|}{TV(u_0)}, \qquad v_0 := u_0 \circ S_0. \tag{4.2}$$

Our numerical results in Figure 4.1 plots the solution computed using the formula (3.6) with the Gaussian initial data

$$u(0,x) = \frac{1}{\sqrt{2\pi}} \exp\Big(-\frac{x^2}{2}\Big). \tag{4.3}$$

As will be explained in the following section, the solution $u = u(t,x)$ is represented by a cloud of points $(S^+(t,y_i), u\circ S^+(t,y_i))_{i=0,\dots,N-1}$, with $y_i = \frac{i+1/2}{N} - \frac{1}{2}$. The simulation is ran with $N = 100$.

Figure 4.1 (a) represents the initial Gaussian condition. Figure 4.1 (b) shows the solution $u(t=3,\cdot)$ during the smooth regime of evolution. Next, Figure 4.1 (c) displays the solution after the shock formation. Finally, Figure 4.1 (d) (at time $t = 106$) demontrates the convergence of the solution toward the so-called N-wave, as expected, which is the asymptotic profile solution $\frac{x}{\sqrt{t}}$ (up to a translation and to a jump). Observe the formation of a "spike" in the shock, which is clearly visible at the time $t = 106$. Namely, our method generates an additional spike within the jump discontinuity (which could be easily filtered and removed, if one wishes). Note also the isolated point in Figure 4.1 (d), which is a minor numerical artifact.

In contrast, Figure 4.2 represents the *conservative solution* with the same initial condition, but computed with our formula (3.5). We can easily deduce this solution from the multivalued one. The solution is selected among all possible values by using the re-ordering map T in the polar factorization (2.1).

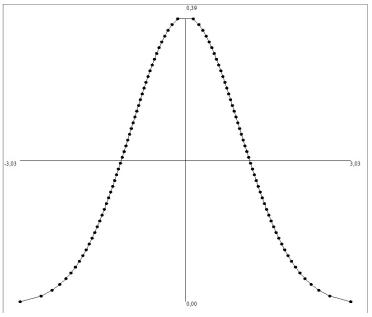

(a) t=0: initial condition

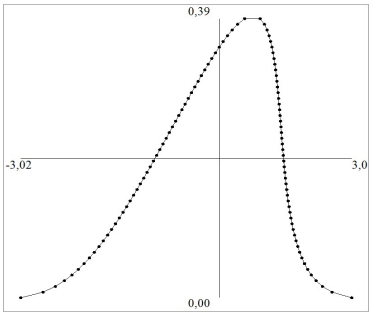

(b) t=3: smooth regime

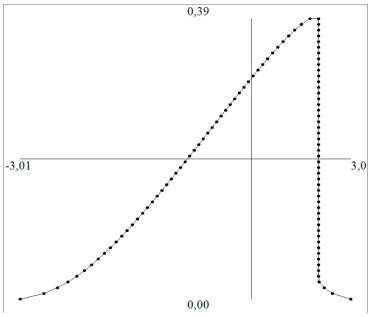

(c)t=6: shock formation

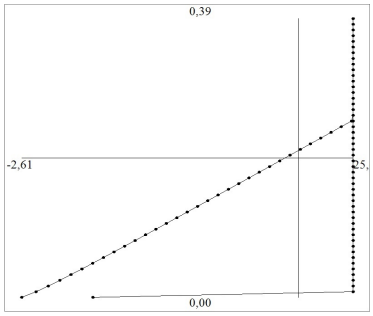

(d) t=106: N-wave regime.

Figure 4.1: Entropy dissipative solutions to Burgers equation

5. Implementation of the convex hull algorithm (CHA)

We now present our algorithm for one-dimensional conservation laws of the form (1.1), that is,

$$\partial_t u + \partial_x f(u) = 0, \qquad u(0,x) = u_0(x), \quad x \in \Omega \subset \mathbb{R}. \tag{5.1}$$

We rely on our formulas (3.6) and (3.5), proposed in the first part of this paper. We introduce the map $S : \Lambda \mapsto \Omega := \mathbb{R}$ by

$$S(t,\cdot) = S_0 + tf'(v_0), \quad S_{0,\#}m = \frac{|\partial_x u_0|}{TV(u_0)}, \quad v_0 := u_0 \circ S_0. \tag{5.2}$$

We are going to our numerical algorithm, step by step, by focusing on Burgers equation, for simplicity in the presentation. The proposed algorithm yields the solution (3.6) or (3.4), and works equally well in any spatial dimension and and with Hamilton-Jacobi equations. We point out that the code based on our method is available [9], so that our results can be easily reproduced by the reader. This algorithm will be tested with more complex case studies in the following section.

We focus on the formula (3.6) and on Burgers equation studied in the previous section. Our construction is as follows: we consider the characteristic map $S(t,\cdot) = S_0 + tf'(v_0) : \Lambda \mapsto \Omega$, where $v_0 := u_0 \circ S_0$ and we set $S(t,\cdot) := \nabla h(t,\cdot)$. For the numerical tests, we will always use $\Lambda = (-\frac{1}{2}, \frac{1}{2})^D$ (with $D = 1$ in this paper) and $\Omega \subset \mathbb{R}^D$. Our *Convex Hull Algorithm* (CHA) amounts to determine the solution

$$u(t,\cdot) = \big(v_0 \circ (S^+)^{-1}\big)(t,\cdot), \tag{5.3}$$

in which

$$S^+(t,\cdot) = \nabla h^+(t,\cdot), \quad h^+(t,\cdot) \text{ convex hull of } h(t,\cdot). \tag{5.4}$$

The main steps of this algorithm are as follows, for each time t :

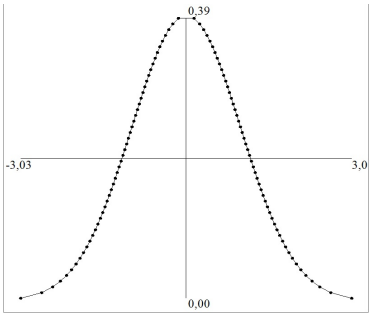

(a) t=0: initial condition

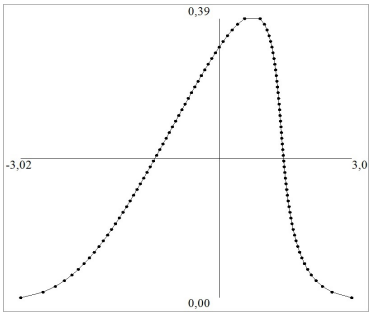

(b) t=3: smooth regime

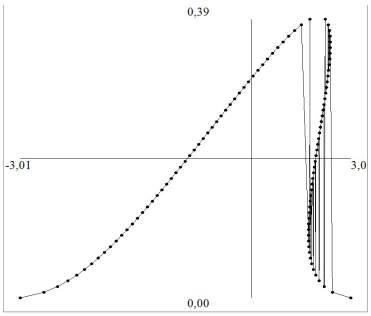

(c) t=6: oscillating regime

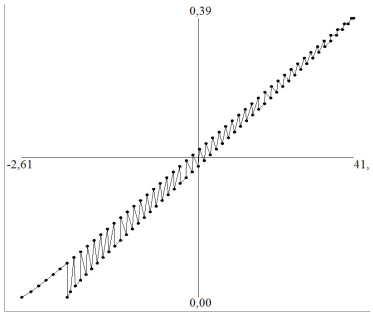

(d) t=106: long time behavior

Figure 4.2: Entropy conservative solutions to Burgers equation

- *Step 1.* Compute the characteristic map $S(t,\cdot)$ (as illustrated by Figure 5.1) and its companion function $h(t,\cdot)$ (see Figure 5.2), deduced coming from of a Helmholtz-Hodge decomposition of the form

$$S(t,\cdot) = (\nabla h + \chi)(t,\cdot), \tag{5.5}$$

  where the map χ is a divergence-free, i.e. $\nabla\cdot\chi = 0$. In one space dimension, we can always normalize χ to vanish identically.

- *Step 2.* Compute the convex hull $h^+(t,\cdot)$ of the function $h(t,\cdot)$. This step is illustrated by Figure 5.3.

- *Step 3.* Compute again the map $S^+(t,\cdot) = \nabla h^+(t,\cdot)$ (see Figure 5.4) as well as the composite function $(u\circ S^+)(t,\cdot) := v_0$ (as represented in Figure 4.1).

Concerning Step 2, efficient algorithms in order to compute convex hulls are available as open source softwares. (See, for instance, http://www.cgal.org.) We used the specialized QHull library available at http://www.qhull.org. Our numerical contribution for the present work is a Helmoltz-Hodge decomposition/re-composition code based on multi-dimensional unstructured meshes, which can be described as follows.

Let us introduce the following non-local basis functions $\psi_Y(X) : \Lambda \mapsto \mathbb{R}$, where $Y = (y_d)_{d=1,\dots,D} \in \Lambda$:

$$\psi_Y(X) = \frac{1}{2}|X-Y|_1 = \frac{1}{2}\sum_{d=1,\dots,D}|x_d - y_d|, \quad X \in \Lambda. \tag{5.6}$$

Let $Y := (Y_n)_{n=1,\dots,N}$, N be distincts sampling points of the computational domain Λ, with $Y_j := \frac{i+1/2}{N} - \frac{1}{2}$ in our one-dimensional setting. We then consider any (possibly) vector-valued map $S : \Lambda \mapsto \Omega$ and the following minimization problem

$$\inf_{(\alpha_n)_{n=1,\dots,N}\in\mathbb{R}^N}\int_\Lambda |S - \sum_{n=1,\dots,N}\alpha_n\nabla\psi_{Y_n}|_2^2\,dm, \tag{5.7}$$

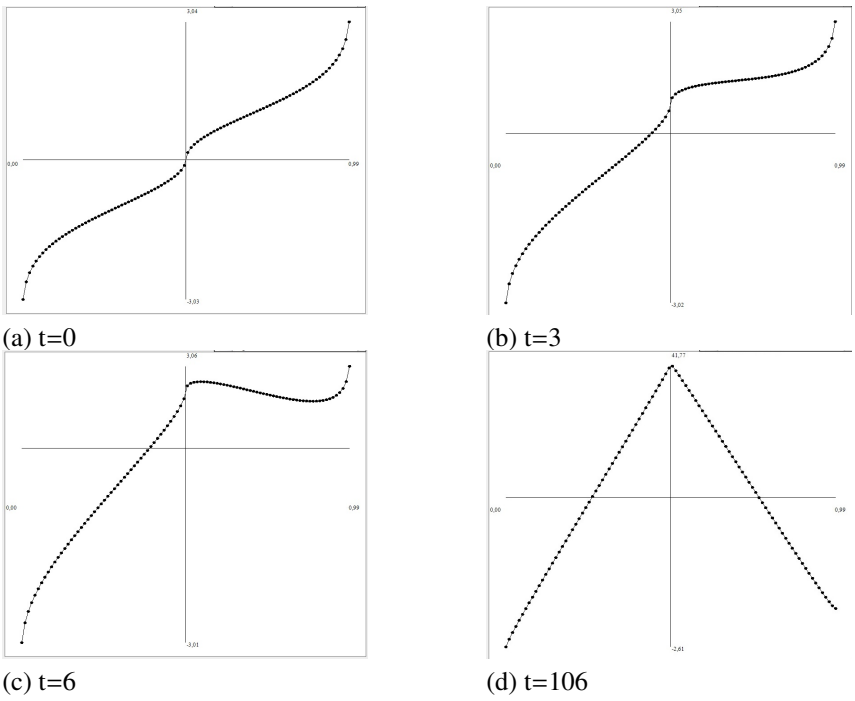

(a) t=0 (b) t=3

(c) t=6 (d) t=106

Figure 5.1: The characteristic map $S(t,\cdot)$

which can be interpreted as a classical projection method. This latter problem is approximated by a linear system corresponding to a Gram-Schmidt algorithm (in which the notation $\langle f,h\rangle_{L^2(\Lambda,\mathbb{R}^D)}$ is used for the integral $\int_\Lambda\langle f_1,f_2\rangle$ of the scalar product of two vector-valued functions):

$$\begin{aligned}&\sum_{j=1,\dots,N}\alpha_n\langle\nabla\psi_{Y_i},\nabla\psi_{Y_j}\rangle_{L^2(\Lambda,\mathbb{R}^D)}=\frac{1}{2}\langle S,\nabla\psi_{Y_i}\rangle_{L^2(\Lambda,\mathbb{R}^D)}\\&\simeq\frac{1}{2N}\sum_{\substack{n=1,\dots,N\\n\neq i}}S(Y_n)\cdot\nabla\psi_{Y_i}(Y_n),\quad i=1,\dots,N.\end{aligned}\tag{5.8}$$

This linear system is invertible, provided $Y_i\neq Y_j, i\neq j$, and the right-hand side approximation makes sense for all maps S that are finite sums of convex and concave functions. Once the coefficients α_n are computed, the component h_Y is obtained by

$$h_Y=\sum_{n=1,\dots,N}\alpha_n\psi_{Y_n}.\tag{5.9}$$

Once the convex hull h_Y^+ is computed, a similar algorithm yields us the components α_n^+ of the projection $h_Y^+=\sum_n\alpha_n^+\psi_{Y_n}$. This allows us to finally compute

$$S_Y^+=\sum_n\alpha_n^+\nabla\psi_{Y_n}.\tag{5.10}$$

6. Applications

6.1. A fluid dynamical problem

Finally, we consider the coupling between Burgers equation satisfied by the velocity function u, that is,

$$\partial_t u+\partial_x\Big(\frac{u^2}{2}\Big)=0\tag{6.1}$$

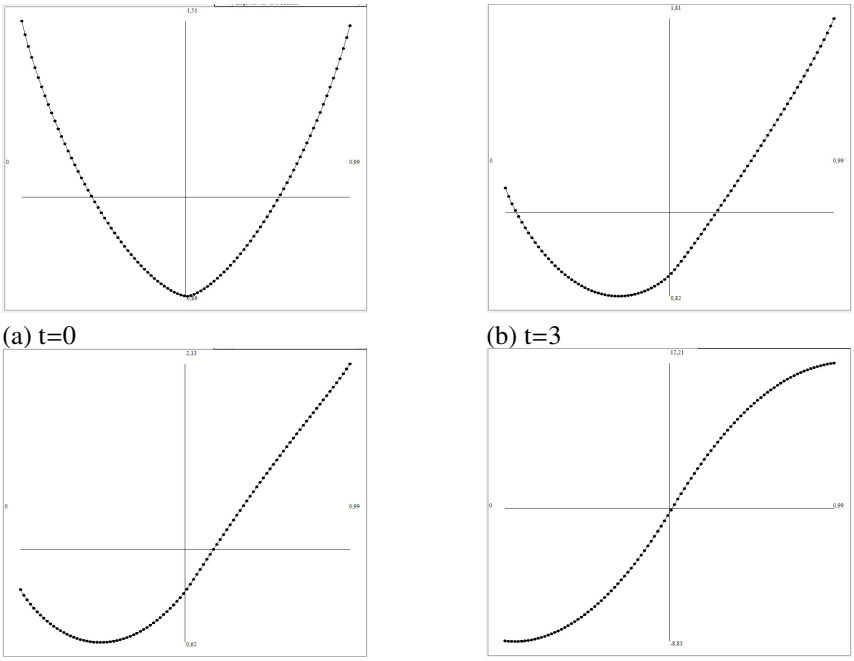

(a) t=0 (b) t=3

(c) t=6 (d) t=106

Figure 5.2: The map $h(t,\cdot)$

and a linear transport equation for a passive scalar w (cf. [7] for a mathematical background):

$$\partial_t w + u\partial_x w = 0. \tag{6.2}$$

By setting $\rho := w_x$, we can interpret (u, w) as solutions to the system of fluid dynamics

$$\partial_t \rho + \partial_x(\rho u) = 0, \tag{6.3}$$

$$\partial_t(\rho u) + \partial_x(\rho u^2) = 0. \tag{6.4}$$

Let $S = S(t,\cdot)$ be the characteristic map for Burgers equation, i.e. $S_t = v_0 = u \circ S$. Consider the function

$$w(t,\cdot) = w(0,\cdot) \circ S(0,\cdot) \circ S(t,\cdot)^{-1} \tag{6.5}$$

with which we can compute (at least formally) $0 = \big(w \circ S\big)_t = w_t \circ S + S_t w_x \circ S = \big(w_t + w_x u\big) \circ S$. Hence, $w_t + w_x f'(u) = 0$, provided S is surjective, so that (6.3)-(6.4) is satisfied. Consequently, we obtain the function associated with the density $w(t,\cdot) = w(0,\cdot) \circ S(0,\cdot) \circ S^{-1}(t,\cdot)$.

Figures 6.1 and 6.2 display the results of our numerical method for this problem. We have plot both $w(t,\cdot)$ and $\rho(t,\cdot)$, where the initial density is taken as

$$\rho(0,x) = \frac{1}{\sqrt{2\pi}} \exp\Big(-\frac{x^2}{2}\Big). \tag{6.6}$$

The velocity $u(t,\cdot)$ follows Burgers equation, and is computed as we explained earlier. (See Figure 4.1 for the velocity at the corresponding times.) Note that the density $\rho(t,\cdot)$ is singular after the shock formation, and we thus performed a suitable truncation in order to display the function $\rho(t,\cdot)$ in Figure 6.2.

6.2. Conservation laws with one inflection point

We next investigate the class of conservation laws of the form (1.1) with non-convex flux. Such laws arise in, for instance, material science or the dynamics complex fluid flows.

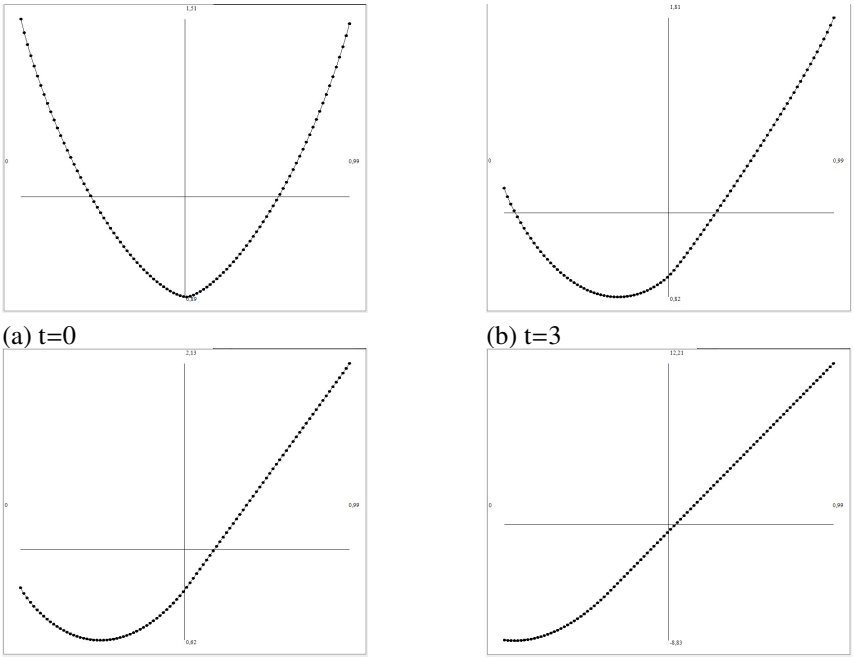

(a) t=0 (b) t=3

(c) t=6 (d) t=106

Figure 5.3: Convex hull transform component $h^+(t,\cdot)$

Specifically, in (5.1), we choose $f(u) = \frac{1}{3}u^3 - u$. The first numerical test corresponds to Riemann data generating a non-monotone shock formation, that is a shock $(u_l, u_m = .25)$ followed by a rarefaction wave $(u_m = .25, u_r)$; see Figure 6.3:

$$u(0,x) = u_l := -0.5 \text{ for } x < 0; \qquad u_r := 0.5 \text{ for } x \geq 0.$$

For our second numerical test, we use an initial data with *two* shocks, which initially separated but interact at a later time. After the interaction, the middle state u_m cancels out and the solution stabilizes to single shock $(u_l = 1., u_r := .25)$ traveling at a negative velocity (cf. Figure 6.4):

$$u(0,x) = u_l := 1. \text{ for } x < -0.5; \quad u_m := -0.5 \text{ for } -0.5 \leq x \leq 0.5;$$

$$u(0,x) = u_r := .25 \text{ for } x \geq 0.5.$$

It is remarkable that, even for such a non-convex flux, our algorithm generates the entropy solution (i.e. physically meaningful) to the problem, which is the one characterized in [5].

6.3. Conservation laws with several inflection points

We finally apply the CHA method to a conservation law whose flux admits several inflection points. Specifically, we consider the nonconvex function

$$f(u) = -u(u-1)(u-2)(u-3)(u-5)/200. \tag{6.7}$$

This example provides us with a further challenge for our method. The first test we consider corresponds to the Riemann data

$$u(0,x) = u_l = 0 \text{ for } x < 0; \qquad u_r := 4.5 \text{ for } x > 0, \tag{6.8}$$

with which the solution is expected to exhibit a rather complex wave pattern, that is, two rarefaction waves and two shocks. The numerical results are strikingly in accordance with the theoretically expected ones; see Figure 6.5.

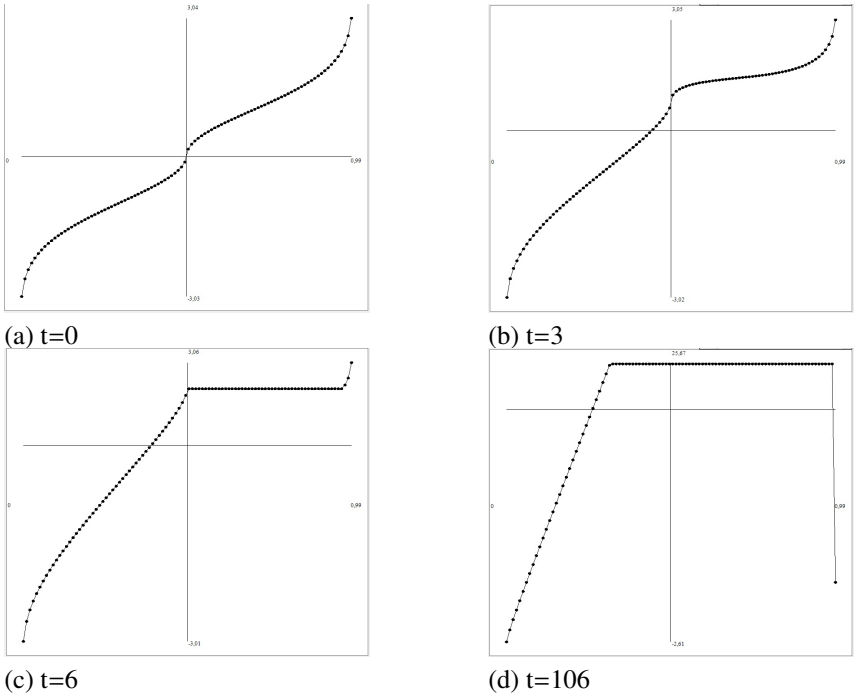

(a) t=0 (b) t=3

(c) t=6 (d) t=106

Figure 5.4: Convex hull transform $S^+(t,\cdot)$

Second, we investigate the time-asymptotic behavior of the CHA-algorithm with the same flux of degre five, but now with a Gaussian initial data (as defined earlier). Even though this data generates a complex wave pattern for sufficiently small times, the solutions are expected to converge toward a generalization of the N-wave of the convex case. Such a kind of convergence is indeed observed with our method, as illustrated by Figure (6.6). Yet, we emphasize the non-trivial shape of the asymptotic N-wave in this case.

7. Concluding remarks

The method proposed in this paper has the following advantages:

- The method applies to hyperbolic problems and Hamilton-Jacobi equations. It generates solutions at any arbitrary time and does not require a time-evolution. In particular, we can easily compute the solutions at an arbitrary large time and therefore determine the asymptotic regime of the solutions (such as the N-wave profile for convex hyperbolic equations).

- The key observation made in this work is that the multivalued solutions contains all the "information" about the entropy dissipative solutions, so that the latter can be recovered from the former by our convex hull algorithm (CHA).

- The jump discontinuities in solutions (shock waves) are sharply represented and described with finitely many points proportionally to the discontinuity strength. This is in contrast with methods based on finite difference schemes for which the numerical solutions contain only a few points within the shocks.

- Especially in a multidimensional setting, the sampling $Y := (Y_n)_{n=1,\dots,N}$ (cf. Section 5) should be chosen to be equidistributed in Λ. Such a set can be computed by a random generator, but a better choice is an optimal quantizer of the "uniform law", which can be achieved when the initial condition is written as a discrete sum of convex and concave components.

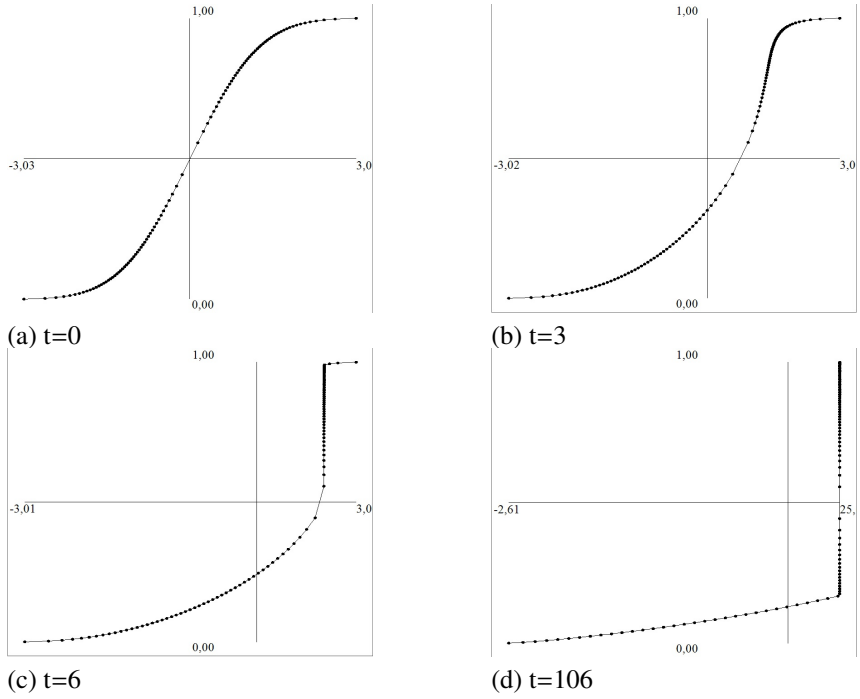

Figure 6.1: Solution component $w(t, \cdot)$

- Optimization strategies can be developed for the proposed algorithm. For instance, removing discrete points lying inside the convex hull and adding discretization points outside. Such a strategy allows for instance to keep the discretization error bounded uniformly in time.

Acknowledgments

The first author (PLF) was partially supported by the Centre National de la Recherche Scientifique (CNRS) and the Agence Nationale de la Recherche through the grants ANR 2006–2-134423 and SIMI-1-003-01.

Bibliography

References

[1] Boscarino S. and Russo G., On a class of uniformly accurate IMEX RungeKutta schemes and application to hyperbolic systems with relaxation, SIAM J. Sci. Comput. 31 (2009), 1926–1945.
[2] Forestier A. and LeFloch P.G., Multivalued solutions to some nonlinear and nonstrictly hyperbolic systems, Japan J. Indus. Appl. Math. 9 (1992), 1–23.
[3] Hopf E., The partial differential equation $u_t + uu_x = u_{xx}$, Comm. Pure Appl. Math. 3 (1950), 201–230.
[4] Jaisankar and Raghurama Rao S.V., A central Rankine-Hugoniot solver for hyperbolic conservation laws, Jour. Comput. Phys. 228 (2009), 770–798.
[5] Kruzkov S.N., First-order quasilinear equations with several space variables, Math. USSR. Sb. 10 (1970), 217–243.
[6] Lax P.D., Hyperbolic systems of conservation laws and the mathematical theory of shock waves, CBMS Regional Conference Series in Mathematics No. 11, Philadelphia, SIAM, 1973.
[7] LeFloch PG., An existence and uniqueness result for two nonstrictly hyperbolic systems, IMA Volumes in Math. and its Appl.,"Nonlinear evolution equations that change type", ed. B.L. Keyfitz and M. Shearer, Springer Verlag, Vol. 27, 1990, pp. 126–138.
[8] LeFloch P.G., Graph solutions to nonlinear hyperbolic systems, J. Hyper. Diff. Equa. 1 (2004), 243–289.
[9] Mercier J.M., A numerical code for nonlinear hyperbolic equations, available at http://www.crimere.com/blog/jean-marc/p=2072.
[10] Sidilkover D. and Karniadakis G.E., Non-oscillatory spectral element Chebyshev method for shock wave calculations, Jour. Comput. Phys. 107 (1993), 10–22.

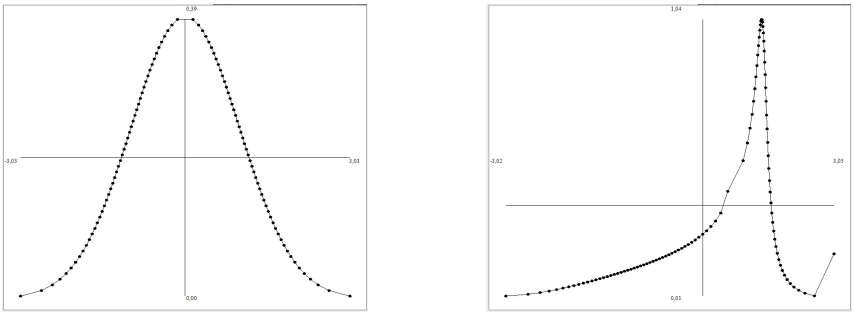

(a) t=0 (b) t=3

(c) t=6 (d) t=106

Figure 6.2: Solution component $\rho(t, \cdot)$

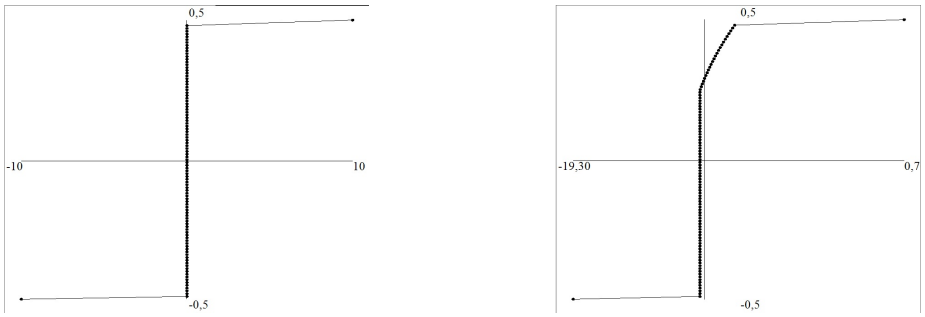

t=0. t=10.

Figure 6.3: Solutions with non-convex flux

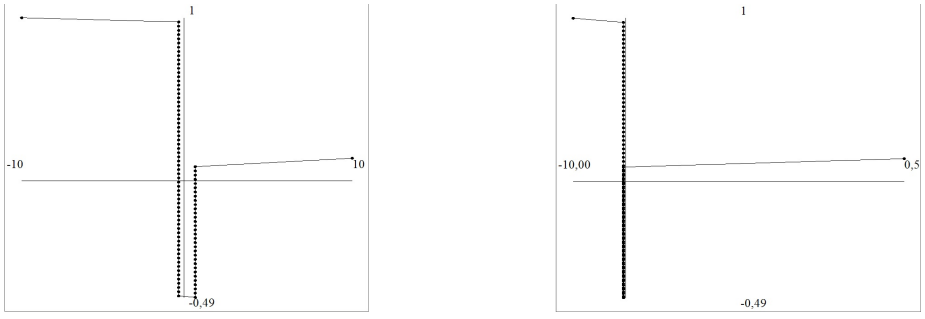

(a) t=0 (b) t=10

Figure 6.4: Shock wave interaction

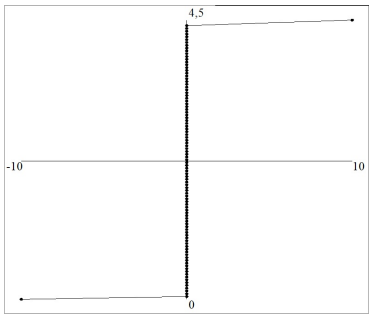

t=0

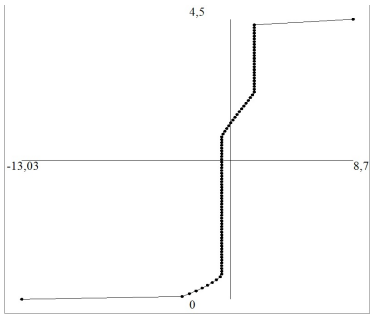

t=20

Figure 6.5: Complex wave pattern for a flux having multiple inflection points

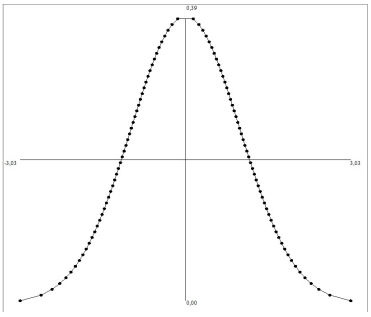

t=0.

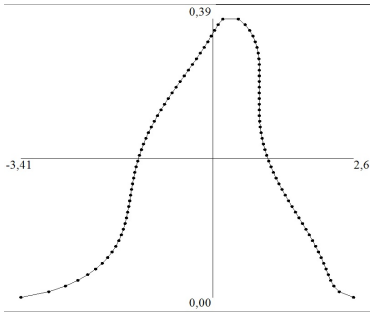

t=.5

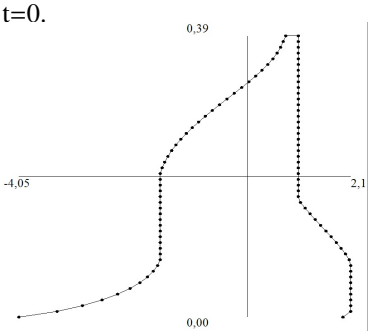

t=1.

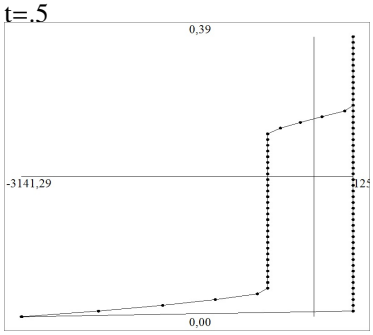

t=1001

Figure 6.6: Asymptotic convergence with a flux having multiple inflection points